Available online at www.sciencedirect.com
SCIENCE DIRECT
Bioorganic & Medicinal Chemistry 14 (2006) 1838–1850
Bioorganic & Medicinal Chemistry

Novel vitamin D_3 antipsoriatic antedrugs: 16-En-22-oxa-1α,25-$(OH)_2D_3$ analogs

Kazuki Shimizu,* Akira Kawase, Tsuyoshi Haneishi, Yasuharu Kato, Takamitsu Kobayashi, Nobuo Sekiguchi, Tessai Yamamoto, Masaki Ishigai, Kazuo Tokuda, Tomochika Matsushita, Shin Shimaoka and Kazumi Morikawa

Fuji Gotemba Research Laboratories, Chugai Pharmaceutical Co., Ltd., 1-135 Komakado, Gotemba, Shizuoka 412-8513, Japan

Received 6 September 2005; revised 19 October 2005; accepted 20 October 2005
Available online 22 November 2005

Abstract—A series of 16-en-22-oxa-derivatives of vitamin D_3 based on the structure of maxacalcitol (**2**) were prepared. Maxacalcitol is currently used topically for the treatment of psoriasis and is recognized as the most successful antedrug of natural vitamin D_3 because it retains the original antiproliferative activity of calcitriol without increased calcemic activity. We introduced 16-olefinic functionality to accelerate the oxidative metabolism of the drug in liver, presumed to be essential for the reduction of calcemic activity, and modified the side-chain moiety by placing the 22-oxygen on the more labile allylic carbon center. Novel 22-oxa analogs (**7a**–**i**), carrying either the 24-alkynyl bond or 24-hydroxy functionality in addition to the 16-double bond were synthesized and their pharmacokinetics were evaluated.

1. Introduction

Since the recognition of the differentiation-inducing activity naturally occurring in the hormone calcitriol (1α,25-dihydroxyvitamin D_3; **1**, Chart 1) was reported in the early 1980s,[1] a number of studies[2] have focused on the separation of the antiproliferation and cell differentiation activities from the undesirable calcemic activity by modification of the natural structure in order to develop a more favorable therapeutic index. Analogs of calcitriol (**1**) such as maxacalcitol (**2**),[3] tacalcitol (**3**),[4] and calcipotriol (**4**)[5] have been developed for treatment of various diseases such as psoriasis, secondary hyperparathyroidism, and osteoporosis by modification of the side-chain moiety of **1** which reduces the competing calcemic activity while retaining non-calcemic activity (Chart 1). However, treatment requires careful administration due to toxicity and a drug with higher efficacy and safety due to reduction of calcemic activity is in demand.

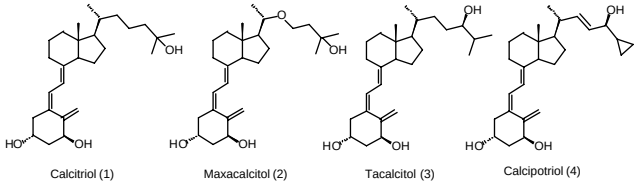

Chart 1. Structures of **1** and its analogs.

Vitamin D analog **2**, currently used for the treatment of psoriasis in ointment form and secondary hyperparathyroidism[6] in injection form, differs from the others in that the 22-methylene functionality is replaced by an oxygen atom. The observed reduction of the calcemic activity of **2** is assumed to be due to the rapid oxidative metabolism by liver CYP[7,8] which converts the absorbed **2** rapidly into the inactive metabolite after exhibiting the desired cell-antiproliferative activity. Maxacalcitol (**2**) is absorbed topically and assumed to be oxidized at the C23 center adjacent to the oxygen atom rapidly after entering into liver through systemic circulation, and gave rise, presumably via the hemiacetal intermediate **5** by liver CYP, to the inactive metabolite **6**[9] (Scheme 1).

With this mode of action of an 'antedrug'[10] or a 'soft drug'[11] in mind, we decided to design a new vitamin

Keywords: 16-En-22-oxa-1α,25-dihydroxyvitamin D_3 analogs; Antedrug; Low calcemic activity; Psoriasis.
* Corresponding author. Tel.: +81 550 87 6723; fax: +81 550 87 5326; e-mail: tazumikzk@chugai-pharm.co.jp

0968-0896/$ - see front matter © 2005 Elsevier Ltd. All rights reserved.
doi:10.1016/j.bmc.2005.10.034

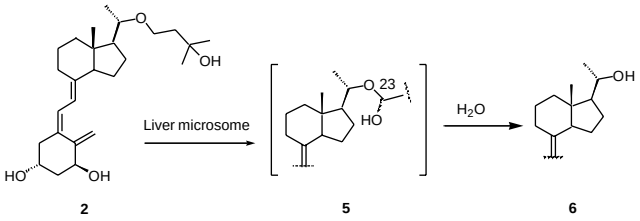

Scheme 1. Postulated metabolic pathway of **2**.

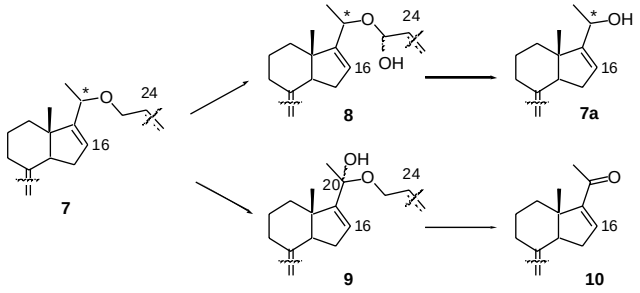

Chart 2. Allylic activation of 22-oxa-vitamin D_3 analogs.

D_3 antedrug[12] based on the structure of **2** that would exhibit a higher pharmacological activity having a lower calcemic activity while preserving its 22-oxa structure to allow faster metabolism. We were most interested in the change of the activities after the modification around the 22-oxygen center and, since it was reported that 16-en-calcitirol[2,13] exhibited a lower calcemic activity while improving differentiation-inducing activity, we designed and prepared the 22-oxa-derivatives **7** with a 16-double bond in order to place the 22-oxygen on the more labile allylic center to reduce the undesirable calcemic activity through faster metabolism in systemic circulation. As in the metabolism of lovastatin[14–16] as well as of quinidine,[17] it is well recognized that an allylic center is susceptible to metabolic oxidation with CYP3A4 in the metabolic pathway. We expected the compounds to be more bio-susceptible with the introduction of a 16-double bond owing to the generation of new allylic centers (Chart 2).

2. Results and discussion

2.1. Chemistry

Synthesis of the newly designed 16-en-22-oxa-vitamin D analogs **7a**–**i** (Scheme 2) was carried out efficiently from the common trienol (*S*)-**13** and its epimer (*R*)-**13**, as developed in our laboratories,[18–21] starting from dehydroandrosterone (**12**). Other than for the design of **7b** and **7i**, a direct alkylation of **13** under standard Williamson conditions furnished the corresponding ether **14**, further transforming into compounds **7c**–**h**, following the procedure developed for the synthesis of **2**, a sequence involving the introduction of 7-olefin functionality, and photochemical and thermal isomerization steps. The presumed metabolite (*S*)-**7a** corresponding to hexanor compound **6** from **2**, as well as its epimer

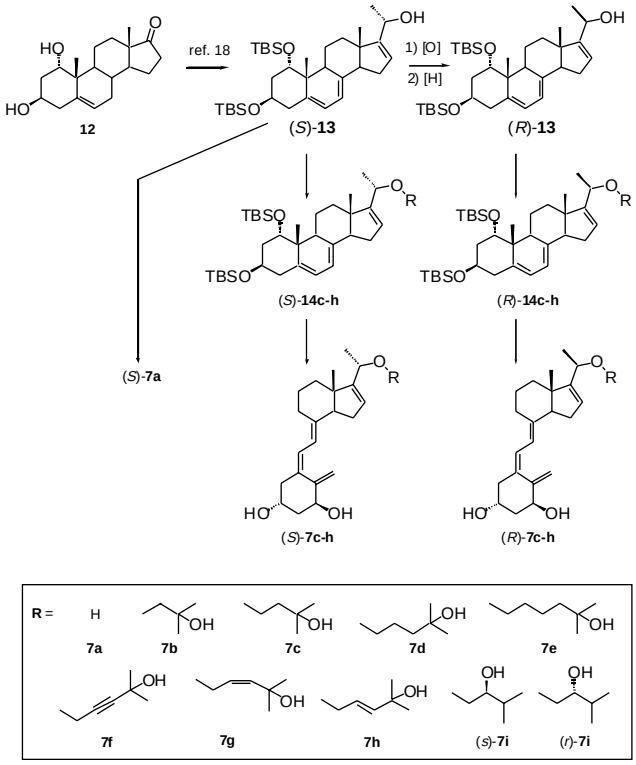

Scheme 2.

(*R*)-**7a**, was prepared from trienol **13** having corresponding stereochemistry using the same procedure without 22-O-alkylation.

As direct construction of the tertiary alcohol **14b** from the precursor **13** by reaction with 1,1-dimethyloxirane was difficult, **13** was treated first with glycidyl tosylate to give the epoxide **15**, which was then transformed into **14b** via the ketone **17** with oxidation followed by reaction with methylmagnesium bromide (Scheme 3).

All four isomers of the compound **7i** having a 24-hydroxy functionality were prepared (Scheme 4) from the precursor **13** from reaction with (*R*)- or (*S*)-1,2-epoxy-3-methylbutane through the corresponding secondary alcohol **19i**, respectively, according to established procedure as shown above.

2.2. Biology

Biological activity of the compounds prepared in the present study was evaluated as follows using **2** as the reference: (i) in vitro metabolic stability, (ii) in vivo calcemic activity, and (iii) in vitro pharmacological activity. For in vitro metabolic stability, the time-dependent residual ratio in rat liver microsome culture was measured to estimate the elimination rate constant, k_e value. The calcemic activity was estimated on the basis of the calcemic increment levels from in vivo rat percutaneous administration. The pharmacological activity was estimated by measurement of

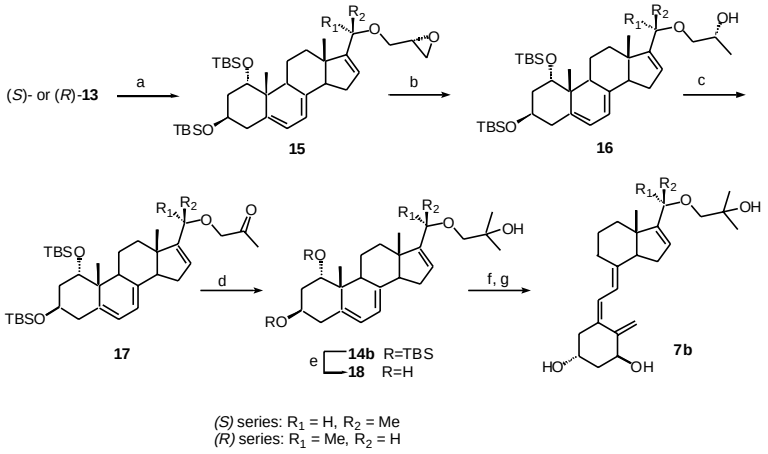

Scheme 3. Reagents and condition: (a) NaH, 15-crown-5, (*R*)-(−)-glycidyl tosylate, THF; (b) LAH, Et_2O; (c) TPAP, NMO, MS4Å, CH_2Cl_2; (d) MeMgBr, THF; (e) TBAF, THF; (f) hν, EtOH; (g) heating.

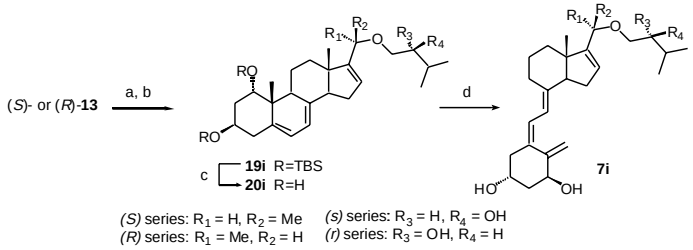

Scheme 4. Reagents and condition: (a) tBuOK, dibenzo-18-crown-6, (*R*)-(−)-1,2-epoxy-3-methylbutane or (*S*)-(+)-1,2-epoxy-3-methylbutane, toluene; (b) TBAF, THF; (c) hν, EtOH; (d) heating.

in vitro human keratinocyte growth inhibitory activity.[22]

Table 1 shows the profile of compounds **7b**–**e** having saturated side chains and **2** and (*S*)-**7a** having no alkyl groups on 22-oxygen. All of the compounds metabolized at a faster rate than **2** with a comparable lower calcemic activity, demonstrating that the introduction of the 16-double bond accelerated the metabolism as expected and, unexpectedly, lessened the stereochemical effect of 20-center. In addition, it was reported that the introduction of the 16-en substructure lessened the binding affinity to DBP (vitamin D binging protein),[23] which might contribute to promoting metabolism. In the evaluation of DBP-binding affinity, affinity lower than that of **2** was observed in all of the analogs (unpublished data). Although the stereochemistry of the 20-center did not have effect on any pharmacological activity in the 16-en compounds, the length of the side chain appeared critical: the longer side chains showed a greater antiproliferative activity.

Table 2 shows the profile of the substrates **7f**–**h** having C24 unsaturation to place the 22-oxygen on the doubly allylic center. Some compounds exhibited a desirable profile with pharmacological activity stronger than that of **2** regardless of the configuration of the C20 center. However, the activity was highly dependent on the configuration of the unsaturated bond.

Regarding metabolic stability, all but (*R*)-**7h** having a 20-*epi*-24(*E*)-ene structure exhibited a better profile than **2**. As expected, the doubly allylated system accelerated metabolism, although it seemed to be highly dependent on the stereochemistry at the C20 center and the olefin configuration at the C24 center. Among the derivatives, (*S*)-**7f** having a 24-yne structure and (*S*)-**7g** having a 24(*Z*)-ene structure exhibited the lowest metabolic stability profiles.

The calcemic activity was similar in all of the compounds and comparable to **2**.

All compounds tested showed stronger antiproliferation activity than **2**. In particular, the 24-yne derivatives (*S*)-**7f** and (*R*)-**7f** and the two C24 olefin isomers (*S*)-**7h** and (*R*)-**7g** exhibited potent activity. This indicates the importance of the steric and configuration environment around the side-chain moiety. Interesting is the stereochemical dependence of the activity in two pairs of the 24-olefinic diastereomers in which (*S*)-**7g** and (*R*)-**7h** exhibited lower activity, suggestive of the ligand structure in the VDR-LBD (ligand binding domain).

Considering all factors, the 24-alkyne derivative having 20(*R*)-configuration (*R*)-**7f** is concluded to have the best profile, greatly exceeding **2** in every respect. Although we did not identify the metabolites indicating oxidation, occurring either at C20 or at C23, the results

Table 1. Biological activity of 16-en-22-oxa-vitamin D_3 analogs **7a–e**

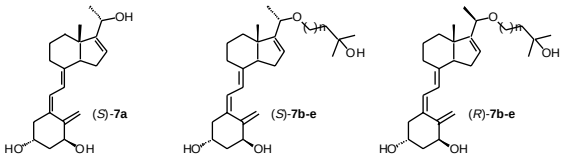

Compound	*n*	Metabolic stability k_e ratio versus **2**[a]	In vivo serum Ca (mmol/L)[b]	Ratio of Ca change to vehicle C (%)[g]	Antiproliferation activity	
					IC_{50} (nM)[h]	A (%) versus **1**[i]
2		1	2.60 ± 0.22[c]	98.5	22.6	120.5
(*S*)-**7a**		5.87	1.40 ± 0.04[d]	0	>1000	2.7
(*S*)-**7b**	0	6.78	1.40 ± 0.04[e]	7.7	548.8	5.0
(*S*)-**7c**	1	1.28	2.16 ± 0.07[e]	66.2	50.4	54.1
(*S*)-**7d**	2	2.07	2.50 ± 0.09[f]	85.2	13.5	202.1
(*S*)-**7e**	3	2.07	2.44 ± 0.03[f]	80.7	14.0	194.2
(*R*)-**7b**	0	4.04	1.37 ± 0.02[e]	5.4	797.9	3.4
(*R*)-**7c**	1	1.47	2.03 ± 0.19[e]	56.2	39.5	69.0
(*R*)-**7d**	2	1.76	2.20 ± 0.16[f]	63.0	20.9	130.3
(*R*)-**7e**	3	13.46	2.57 ± 0.14[f,j]	90.4	7.5	362.0

[a] Metabolic stability was calculated as the ratio of the k_e value of the analog to **2**.
[b] The in vivo calcemic activity of the test compounds determined by measuring the serum calcium level in mice after single percutaneous administration.
[c] Vehicle levels (mmol/L): 1.31 ± 0.04.
[d] Vehicle levels (mmol/L): 1.44 ± 0.03.
[e] Vehicle levels (mmol/L): 1.30 ± 0.05.
[f] Vehicle levels (mmol/L): 1.35 ± 0.02.
[g] Calcemic activity (%) = {(blood ionized Ca [mmol/L] of the analogs) − (blood ionized Ca [mmol/L] of the vehicle)}/(blood ionized Ca [mmol/L] of the vehicle) × 100.
[h] The in vitro effect is expressed as percentage activity at IC_{50} (n = 2, mean value) in comparison with **1**. IC_{50} is the molar concentration of the test compound that causes 50% of the maximal inhibition of proliferation by suppression of [^{3}H]TdR uptake. IC_{50} (nM) of **1**: 27.3 (nM).
[i] Antiproliferation activity (%) = {(IC_{50} [nM] of **1**)/(IC_{50} [nM] of the analogs)} × 100.
[j] We could not reason the observed discrepancy in calcemic activity.

Table 2. Biological activity of 16-en-22-oxa-vitamin D_3 analogs **7f–h**

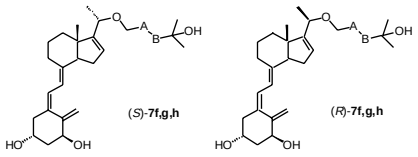

Compound	A–B	Metabolic stability k_e ratio versus **2**[a]	In vivo serum Ca (mmol/L)[b]	Ratio of Ca change to vehicle C (%)[h]	Antiproliferation activity	
					IC_{50} (nM)[i]	A (%) versus **1**[j]
2		1	2.60 ± 0.22[c]	98.5	22.6	120.5
(*S*)-**7f**	yne	5.48	2.44 ± 0.18[d,k]	86.3	3.5	779.5
(*S*)-**7g**	*cis*-ene	5.54	2.63 ± 0.07[d,k]	100.8	12.7	215.2
(*S*)-**7h**	*trans*-ene	3.33	2.36 ± 0.25[e]	76.1	4.8	574.2
(*R*)-**7f**	yne	1.90	2.11 ± 0.18[f]	61.1	5.7	479.8
(*R*)-**7g**	*cis*-ene	3.15	2.56 ± 0.04[g]	89.6	7.5	365.5
(*R*)-**7h**	*trans*-ene	0.90	1.94 ± 0.17[e,k]	44.8	16.5	165.4

[a] Metabolic stability was calculated as the ratio of the k_e value of the analog to **2**.
[b] The in vivo calcemic activity of the test compounds determined by serum calcium levels in mice after single percutaneous administration.
[c] Vehicle levels (mmol/L): 1.31 ± 0.04.
[d] Vehicle levels (mmol/L): 1.31 ± 0.06.
[e] Vehicle levels (mmol/L): 1.34 ± 0.03.
[f] Vehicle levels (mmol/L): 1.31 ± 0.05.
[g] Vehicle levels (mmol/L): 1.35 ± 0.01.
[h] Calcemic activity (%) = {(blood ionized Ca [mmol/L] of the analogs) − (blood ionized Ca [mmol/L] of the vehicle)}/(blood ionized Ca [mmol/L] of the vehicle)} × 100.
[i] The in vitro effect is expressed as percentage activity at IC_{50} (n = 2, mean value) in comparison with **1**. The IC_{50} is the molar concentration of the test compound that causes 50% of the maximal inhibition of proliferation by suppression of [^{3}H]TdR uptake. IC_{50} of **1** was 27.3 (nM).
[j] Antiproliferation activity (%) = {(IC_{50} [nM] of **1**)/(IC_{50} [nM] of the analogs)} × 100.
[k] We could not reason the observed discrepancy in calcemic activity.

indicate metabolism faster than that of **2** in all compounds by introduction of unsaturation at the C24 center.

Table 3 shows the profile of two pairs of 24-hydroxylated diastereomers **7i**, similar to **3** and **4**, without the C25 tertiary hydroxy functionality of **2**. The profiles of the compounds exceeded **2** in most respects.

All of them showed a metabolic stability lower profile than that of **2**. The calcemic profile of these compounds was better than **2** and even better than those of compounds **7f**–**h** with unsaturation at the C24 center (Table 2), suggesting the importance of C24 hydroxy functionality in the metabolism. The antiproliferative activity, on the other hand, was almost comparable to **2**, with the exception of 20(*S*)-isomers (*Sr*)-**7i** and (*Ss*)-**7i** which exhibited 3–4 times lower activity. This observation is of particular interest as the presence of a C24 hydroxy functionality seemed to be critical for a faster metabolism and 24(*R*) configuration tended to contribute to metabolism only slightly. It has been postulated that the metabolism of **1** in kidney starts from the oxidation at the C24 center by 24-hydroxylase leading to inactive calcitroic acid by stepwise cleavage of the side chain and it seemed to be the same with our compounds. Therefore, 24-hydroxy modification weakens the calcemic action of **2** through promotion of 23-oxidative metabolism next to the 24-hydroxy group that increases affinity to the metabolic enzyme, while retaining the activity almost equivalent to that of **2**.

In addition to the metabolic effect mentioned above, pharmacodynamics were also considered as an explanation for the profiles of the analogs. The reduction of calcemic activity with non-calcemic activity retention in 24-hydroxy analogs, like **3** and **4**, compared with that of 25-hydroxyl analogs might be due to the different hydrogen bonding with VDR of these two types of compounds. Moreover, as it appeared in **7i**, the 24-hydroxy functionality and 22-oxygen atom might have an intramolecular hydrogen-bonding interaction. These differences might affect sequential transcriptional events such as the interaction with co-factors.[24]

Table 4 shows the in vivo pharmacokinetic data of two 20-diastereomers of C24-hydroxy compounds, (*Ss*)-**7i** and (*Rs*)-**7i**, and the 24-alkyne (*R*)-**7f**, administered intravenously to rats. It can be seen that total body clearance values (CL_{tot}) of these compounds were 2.4-3.5 times higher than that of **2**, which indicates rapid disappearance from the systemic circulation. The profiles suggest that these compounds exhibited activity in skin first and were then taken into systemic circulation with rapid conversion into inactive metabolites through possibly side-chain cleavage.

Table 4. Pharmacokinetic parameters of 16-en-22-oxa-vitamin D_3 analogs **7f** and **7i** in rat

Compound	Dose (μg/kg)	CL_{tot}[b] (mL/h/kg)
2	10	855
(*Ss*)-**7i**	10	2958
(*Rs*)-**7i**	100[a]	2093
(*R*)-**7f**	10	2647

[a] Due to detection limitations, a higher dosage was used for the pharmacokinetics of (*Rs*)-**7i**.
[b] Each value represents the mean of 2–4 rats.

Table 3. Biological activity of 16-en-22-oxa-vitamin D_3 analogs **7i**

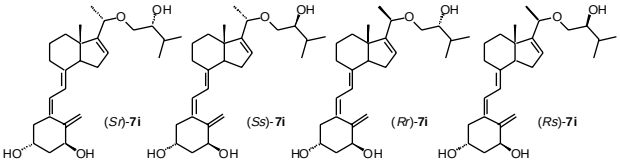

Compound	Metabolic stability k_e ratio versus **2**[a]	In vivo serum Ca (mmol/L)[b]	Ratio of Ca change to vehicle C (%)[f]	Antiproliferation activity	
				IC_{50} (nM)[g]	A (%) versus **1**[h]
2	1	2.60 ± 0.22[c]	98.5	22.6	120.5
(*Sr*)-**7i**	7.51	1.79 ± 0.10[d]	37.7	77.1	35.4
(*Ss*)-**7i**	4.81	2.10 ± 0.08[d]	61.5	60.6	45.1
(*Rr*)-**7i**	4.61	1.76 ± 0.07[e]	30.4	44.4	61.4
(*Rs*)-**7i**	3.04	1.70 ± 0.10[e]	25.9	41.8	65.3

[a] Metabolic stability was calculated as the ratio of the k_e value of the analog to **2**.
[b] The in vivo calcemic activity of the test compounds determined by measuring the serum calcium level in mice after single percutaneous administration.
[c] Vehicle levels (mmol/L): 1.31 ± 0.04.
[d] Vehicle levels (mmol/L): 1.30 ± 0.05.
[e] Vehicle levels (mmol/L): 1.35 ± 0.01.
[f] Calcemic activity (%) = {(blood ionized Ca [mmol/L] of the analogs) − (blood ionized Ca [mmol/L] of the vehicle)}/(blood ionized Ca [mmol/L] of the vehicle) × 100.
[g] The in vitro effect is expressed as percentage activity at IC_{50} (n = 2, mean value) in comparison with **1**. The IC_{50} is the molar concentration of the test compound that causes 50% of the maximal inhibition of proliferation by suppression of [^{3}H]TdR uptake. IC_{50} (nM) of **1**: 27.3 (nM).
[h] Antiproliferation activity (%) = {(IC_{50} [nM] of **1**)/(IC_{50} [nM] of the analogs)} × 100.

From the SAR analysis of **7b–e**, a tendency that a longer side chain increases antiproliferative activity can be seen. In Figure 1, the relative potency of the antiproliferative activities is plotted against the number of carbon atoms in the C20–C25 side chain.

A good correlation was observed between the length of the side chain and the antiproliferation of analogs **7b–e** with a saturated side chain. In the case of 24-hydroxy analog **7i**, the activity was almost comparable to that of **7c**, which suggests that the terminal hydrophobic group is more important for non-calcemic activity than the position of the hydroxyl group. After the introduction of an unsaturated bond into the side chain, **7f–h** exhibited much higher activity than those of corresponding saturated analogs of **7d**. A contributory cause of this improvement was considered to be the reduction of the entropy loss by the configuration fixation on binding. Concerning the level of activity in general, the 24-yn analogs of **7f** showed an extremely strong activity, next were the 24-en analogs of **7g** and **7h**, and last, **7d** showed the lowest activity among these compounds. However, the activity of (*S*)-**7g** and (*R*)-**7h** had no effect on the entropic energy contribution. We speculated that the reason for the differences between the **7g** and **7h** groups is the different binding mode to the VDR. In order to investigate the docking mode, we conducted docking experiments for the **7g** and **7h** ligands, and calculated their torsion angle defined by the atoms C20, C22, C23, and C24. Stereoview of four double bond analogs in stick model, (S)-7**g**, (*R*)-**7h**, (*R*)-**7g**, and (*S*)-**7h**, docked into the binding site of VDR. In this model, the VDR is represented as a Connolly surface (cyan). Hydrogen atoms of each ligand are omitted for clarity. From the four docking models of **7g** and **7h**, the weaker activity analogs, (*S*)-**7g** and (*R*)-**7h**, have orthogonal torsion angles ((*S*)-**7g**, −68.3°; (*R*)-**7h**, 81.9°), while the stronger analogs (*S*)-**7h** and (*R*)-**7g** have anti-configuration ((*S*)-**7h**, −191.1°; (*R*)-**7g**, 177.2°) as shown in Figure 2. Therefore, it was suggested that (*S*)-**7g** and (*R*)-**7h** might bind to VDR with an energetically unfavorable configuration compared to (*S*)-**7h** and (*R*)-**7g**.

From the results shown in Tables 1–4, our intention to make an effective antedrug by separation of the specific activities has been realized. Namely, the introduction of

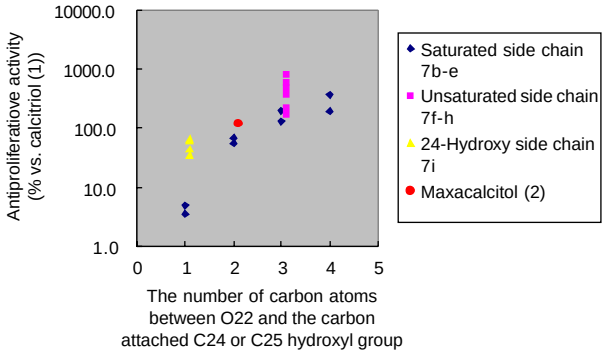

Figure 1. The relationship between the length of the side chain and antiproliferative activity.

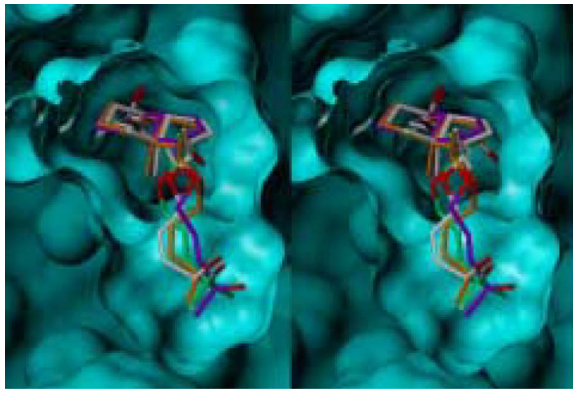

Figure 2. Stereoview of the docking model in VDR of the degree of the dihedral angles between C22 and C23 for (*S*)-**7g** (orange), (*R*)-**7g** (white), (*S*)-**7h** (purple), and (*R*)-**7h** (green).

the 16-double bond into **2**, in addition to an appropriate modification of the side-chain moiety, afforded biologically more susceptible analogs exerting locally acting antiproliferation activity without exerting systemically acting calcemic activity through facile metabolization. The results also suggest the importance of the steric environment around the side-chain moiety of sp, sp^2, and sp^3 centers, and the nature of the substituents as well as the size of the side chain; however, only a hydroxy functionality was examined in the present study.

3. Conclusion

Our intention to develop a more efficient and safe antedrug for the treatment of psoriasis has been realized by modification of the currently used **2** into a more biosusceptible structure. Introduction of the 16-double bond and modification of the side-chain moiety of **2**, while preserving its 22-oxa structure, brought about acceleration of metabolism after entrance into systemic circulation and led to the discovery of some promising derivatives exhibiting better keratinocyte proliferation activity with calcemic activity lower than that of **2**. The present study also provided clarification for the importance of steric factors involving sp, sp^2, and sp^3 centers around the side-chain moiety in creating a better antedrug. On the basis of the present study, we are currently seeking a new derivative with faster metabolism and retention of high proliferation activity to allow a safer, high-dose topical administration.

4. Experimental

4.1. Chemistry: instruments and analyses

Column chromatography was carried out on Wako-gel C-200 (70–230 mesh) purchased from Wako Pure Chemical Industries (Osaka, Japan). Thin-layer chromatography was performed on Merck Kieselgel F^{254} plates. Infrared spectra were obtained using HORIBA FT-730 spectrophotometers. ^1H NMR spectra were recorded on JEOL EX-270 (270 MHz) or VARIAN Gemini-300

(300 MHz) spectrometers using $CDCl_3$ as a solvent. Chemical shifts are reported in parts per million (ppm) downfield from tetramethylsilane or calibrated from $CHCl_3$. Mass spectra (MS) and LC-MS analyses were measured with Shimadzu GCMS QP-1000 (EI), and Waters micromass ZQ 2000 (electrospray ionization method (ESI)) instruments using a 2525BGM pump and a 2996 PDA photodiode array set at 210–400 nm with the MS detection. Analytical HPLC analyses were performed using the following conditions: column A, Inertsil Diol 4.6 × 150 mm column; solvent A, *n*-hexane; solvent B, EtOH; flow rate = 1.0 mL/min; linear gradient time = 15 min; start %B = 5, final %B = 100; or column B, CAPCELLPAK C18 MG2 4.6 × 50 mm column; solvent C, 10 mM aqueous ammonium acetate solution; solvent D, MeOH; flow rate = 1.0 mL/min; linear gradient time = 9.5 min; start %D = 5, final %D = 100. Ultraviolet (UV) spectra were obtained with a Shimadzu UV-1600PC instrument using ethanol as a solvent. High resonance mass spectra (HRMS) were recorded by a Micromass Q-Tof Ultima API mass spectrometer. All reactions were carried out under an atmosphere of argon or nitrogen unless otherwise noted. All extracts were dried over $MgSO_4$ and evaporated under reduced pressure with a rotary evaporator.

4.1.1. 1α,3β-Dihydroxy-20(*S*)-(3-hydroxy-3-methylbutyloxy)-9,10-secopregna-5,7,10(19),16-tetraene ((*S*)-7c). Prepared according to the previous procedure for **2**.[18–21] IR (neat): 3400, 2980, 2940, 1445, 1370, 1165, 1060 cm^{-1}; ^1H NMR (270 MHz, $CDCl_3$): δ 0.78 (s, 3H), 1.23 (s, 3H), 1.24 (s, 3H), 1.31 (d, J = 6.4 Hz, 3H), 2.75–2.90 (m, 1H), 3.47–3.58 (m, 1H), 3.63 (br s, 1H), 3.61–3.73 (m, 1H), 3.91 (q, J = 6.4 Hz, 1H), 4.18–4.30 (m, 1H), 4.39–4.51 (m, 1H), 5.01 (s, 1H), 5.34 (s, 1H), 5.59 (br s, 1H), 6.10 (d, J = 11.4 Hz, 1H), 6.37 (d, J = 11.4 Hz, 1H); MS (ESI): m/z 439 ($[M+Na]^+$); UV λ_{max}: 263 nm; HPLC t_R = 11.08 min (purity 96.9%, column A), HPLC t_R = 10.01 min (purity >99%, column B); HRMS Calcd for $C_{26}H_{40}O_4Na$: 439.2824. Found: 439.2823.

4.1.2. 1α,3β-Dihydroxy-20(*R*)-(3-hydroxy-3-methylbutyloxy)-9,10-secopregna-5,7,10(19),16-tetraene ((*R*)-7c). Prepared according to the procedure for (*S*)-**7c**.[18] IR (neat): 3380, 2940, 2850, 1450, 1370, 1160, 1055 cm^{-1}; ^1H NMR (270 MHz, $CDCl_3$): δ 0.75 (s, 3H), 1.23 (s, 3H), 1.24 (s, 3H), 1.32 (d, J = 6.4 Hz, 3H), 2.75–2.89 (m, 1H), 3.58 (br s, 1H), 3.65 (t, J = 5.8 Hz, 2H), 3.97 (q, J = 6.4 Hz, 1H), 4.20–4.30 (m, 1H), 4.40–4.51 (m, 1H), 5.01 (s, 1H), 5.33 (s, 1H), 5.62 (br s, 1H), 6.10 (d, J = 11.4 Hz, 1H), 6.37 (d, J = 11.4 Hz, 1H); MS (ESI): m/z 439 ($[M+Na]^+$); UV λ_{max}: 264 nm; HPLC t_R = 11.11 min (purity 98.4%, column A), HPLC t_R = 9.82 min (purity >99%, column B); HRMS Calcd for $C_{26}H_{40}O_4Na$: 439.2824. Found: 439.2830.

4.1.3. 1α,3β-Dihydroxy-20(*S*)-(4-hydroxy-4-methylpentyl oxy)-9,10-secopregna-5,7,10(19),16-tetraene ((*S*)-7d). Prepared according to the procedure for (*S*)-**7c**.[18] ^1H NMR (270 MHz, $CDCl_3$): δ 0.77 (s, 3H), 1.21 (s, 6H), 1.29 (d, J = 6.6 Hz, 3H), 2.74–2.90 (m, 1H), 3.19–3.34 (m, 1H), 3.35–3.52 (m, 1H), 3.89 (q, J = 6.6 Hz, 1H), 4.14–4.31 (m, 1H), 4.36–4.51 (m, 1H), 5.00 (s, 1H), 5.33 (s, 1H), 5.57 (br s, 1H), 6.10 (d, J = 11.4 Hz, 1H), 6.36 (d, J = 11.4 Hz, 1H); MS (ESI): m/z 453 ($[M+Na]^+$); UV λ_{max}: 264 nm; HPLC t_R = 11.19 min (purity 96.1%, column A), HPLC t_R = 10.32 min (purity >99%, column B); HRMS Calcd for $C_{27}H_{42}O_4Na$: 453.2981. Found: 453.2968.

4.1.4. 1α,3β-Dihydroxy-20(*R*)-(4-hydroxy-4-methylpentyl oxy)-9,10-secopregna-5,7,10(19),16-tetraene ((*R*)-7d). Prepared according to the previous procedure for (*S*)-**7c**.[18] ^1H NMR (270 MHz, $CDCl_3$): δ 0.74 (s, 3H), 1.21 (s, 6H), 1.31 (d, J = 6.3 Hz, 3H), 2.52–2.67 (m, 1H), 2.76–2.88 (m, 1H), 3.33–3.51 (m, 2H), 3.95 (q, J = 6.3 Hz, 1H), 4.16–4.30 (m, 1H), 4.39–4.50 (m, 1H), 5.01 (s, 1H), 5.33 (s, 1H), 5.61 (br s, 1H), 6.10 (d, J = 11.4 Hz, 1H), 6.37 (d, J = 11.4 Hz, 1H); MS (ESI): m/z 453 ($[M+Na]^+$); UV λ_{max}: 264 nm; HPLC t_R = 11.22 min (purity 98.1%, column A), HPLC t_R = 10.14 min (purity >99%, column B); HRMS Calcd for $C_{27}H_{42}O_4Na$: 453.2981. Found: 453.2964.

4.1.5. 1α,3β-Dihydroxy-20((*S*)-(5-hydroxy-5-methylhexyl oxy)-9,10-secopregna-5,7,10(19),16-tetraene ((*S*)-7e). Prepared according to the procedure for (*S*)-**7c**.[18] IR (neat): 3417, 2968, 2933, 2854, 1446, 1367, 1159, 1099, 1057 cm^{-1}; ^1H NMR (270 MHz, $CDCl_3$): δ 0.74 (s, 3H), 1.21 (s, 6H), 1.30 (d, J = 6.6 Hz, 3H), 2.75–2.88 (m, 1H), 3.40 (t, J = 6.4 Hz, 2H), 3.93 (q, J = 6.6 Hz, 1H), 4.16–4.30 (m, 1H), 4.38–4.51 (m, 1H), 5.02 (s, 1H), 5.34 (s, 1H), 5.60 (br s, 1H), 6.10 (d, J = 11.4 Hz, 1H), 6.38 (d, J = 11.4 Hz, 1H); MS (ESI): m/z 467 ($[M+Na]^+$); UV λ_{max}: 264 nm; HPLC t_R = 11.18 min (purity 99.2%, column A), HPLC t_R = 10.42 min (purity >99%, column B); HRMS Calcd for $C_{28}H_{44}O_4Na$ 467.3137, Found: 467.3139.

4.1.6. 1α,3β-Dihydroxy-20(*R*)-(5-hydroxy-5-methylhexyloxy)-9,10-secopregna-5,7,10(19),16-tetraene ((*R*)-7e). Prepared according to the procedure for (*S*)-**7c**.[18] IR (neat): 3383, 2968, 2933, 2852, 1444, 1367, 1159, 1103, 1055 cm^{-1}; ^1H NMR (270 MHz, $CDCl_3$): δ 0.78 (s, 3H), 1.21 (s, 6H), 1.30 (d, J = 6.6 Hz, 3H), 2.75–2.90 (m, 1H), 3.20–3.34 (m, 1H), 3.34–3.47 (m, 1H), 3.88 (q, J = 6.6 Hz, 1H), 4.15–4.30 (m, 1H), 4.33–4.50 (m, 1H), 5.01 (s, 1H), 5.34 (s, 1H), 5.56 (br s, 1H), 6.11 (d, J = 11.2 Hz, 1H), 6.37 (d, J = 11.2 Hz, 1H); MS (ESI): m/z 467 ($[M+Na]^+$); HPLC t_R = 11.17 min (purity 98.3%, column A), HPLC t_R = 10.54 min (purity >99%, column B); HRMS Calcd for $C_{28}H_{44}O_4Na$ 467.3137. Found: 467.3127.

4.1.7. 1α,3β-Dihydroxy-20((*S*)-(4-hydroxy-4-methyl-2-pentynyloxy)-9,10-secopregna-5,7,10(19),16-tetraene ((*S*)-7f). Prepared according to the procedure for (*S*)-**7c**.[18] IR (neat): 3369, 2929, 2852, 1442, 1369, 1234, 1167, 1060 cm^{-1}; ^1H NMR (270 MHz, $CDCl_3$): δ 0.79 (s, 3H), 1.33 (d, J = 6.6 Hz, 3H), 1.52 (s, 6H), 4.03 (d, J = 15.4 Hz, 1H), 4.14 (m, 1H), 4.15 (d, J = 15.4 Hz, 1H), 4.19–4.30 (m, 1H), 4.41–4.51 (m, 1H), 5.02 (br s, 1H), 5.34 (br s, 1H), 5.62 (br s, 1H), 6.11 (d, J = 11.2 Hz, 1H), 6.38 (d, J = 11.2 Hz, 1H); MS (ESI): m/z 449 ($[M+Na]^+$); UV: λ_{max} 264 nm; HPLC t_R = 11.73 min (purity 98.1%, column A), HPLC

t_R = 9.74 min (purity >99%, column B); HRMS Calcd for $C_{27}H_{38}O_4Na$: 449.2668. Found: 449.2660.

4.1.8. 1α,3β-Dihydroxy-20(*S*)-{(*Z*)-(4-hydroxy-4-methyl-2-pentenyloxy)}-9,10-secopregna-5,7,10(19),16-tetraene ((*S*)-7g). Prepared according to the previous procedure for (*S*)-**7c**.[18] IR (neat): 3369, 2972, 2929, 2850, 1446, 1371, 1169, 1055 cm^{-1}; ^1H NMR (270 MHz, $CDCl_3$): δ 0.78 (s, 3H), 1.34 (s, 6H), 2.54–2.68 (m, 1H), 2.75–2.88 (m, 1H), 3.95–4.30 (m, 4H), 4.38–4.50 (m, 1H), 5.01 (br s, 1H), 5.34 (br s, 1H), 5.44 (dt, J = 12.2, 5.6 Hz, 1H), 5.58–5.70 (m, 2H), 6.11 (d, J = 11.2 Hz, 1H), 6.37 (d, J = 11.2 Hz, 1H); MS (ESI): m/z 451 ($[M+Na]^+$); UV λ_{max}: 263 nm; HPLC t_R = 11.12 min (purity 98.0%, column A), HPLC t_R = 10.16 min (purity >99%, column B); HRMS Calcd for $C_{27}H_{40}O_4Na$: 451.2824. Found: 451.2814.

4.1.9. 1α,3β-Dihydroxy-20((*S*)-(*E*)-(4-hydroxy-4-methyl-2-pentenyloxy)-9,10-secopregna-5,7,10(19),16-tetraene ((*S*)-7h). Prepared according to the procedure for (*S*)-**7c**.[18] IR (neat): 3400, 2929, 2850, 1446, 1369, 1220, 1153, 1101, 1055 cm^{-1}; ^1H NMR (270 MHz, $CDCl_3$): δ 0.79 (s, 3H), 1.33 (s, 6H), 3.81 (dd, J = 6.3, 5.6 Hz, 1H), 3.89–4.04 (m, 2H), 4.17–4.30 (m, 1H), 4.38–4.50 (m, 1H), 5.02 (br s, 1H), 5.34 (s, 1H), 5.59 (br s, 1H), 6.11 (d, J = 11.2 Hz, 1H), 6.27 (d, J = 11.2 Hz, 1H); MS (ESI): m/z 451 ($[M+Na]^+$); UV λ_{max}: 264 nm; HPLC t_R = 11.42 min (purity 95.9%, column A), HPLC t_R = 9.97 min (purity >99%, column B); HRMS Calcd for $C_{27}H_{40}O_4Na$: 451.2824. Found: 451.2818.

4.1.10. 1α,3β-Dihydroxy-20(*R*)-(4-hydroxy-4-methyl-2-pentynyloxy)-9,10-secopregna-5,7,10(19),16-tetraene ((*R*)-7f). Prepared according to the procedure for (*S*)-**7c**.[18] IR (neat): 3400, 2976, 2929, 2852, 1444, 1373, 1234, 1167, 1063 cm^{-1}; ^1H NMR (270 MHz, $CDCl_3$): δ 0.75 (s, 3H), 1.33 (d, J = 6.3 Hz, 3H), 1.52 (s, 6H), 2.55–2.66 (m, 1H), 2.76–2.86 (m, 1H), 4.03–4.31 (m, 4H), 4.40–4.50 (m, 1H), 5.01 (br s, 1H), 5.34 (br s, 1H), 5.56 (br s, 1H), 6.11 (d, J = 11.2 Hz, 1H), 6.37 (d, J = 11.2 Hz, 1H); MS (ESI): m/z 449 ($[M+Na]^+$); UV λ_{max}: 264 nm; HPLC t_R = 11.78 min (purity 98.2%, column A), HPLC t_R = 9.62 min (purity >99%, column B); HRMS Calcd for $C_{27}H_{38}O_4Na$: 449.2668. Found: 449.2685.

4.1.11. 1α,3β-Dihydroxy-20(*R*)-{(*Z*)-(4-hydroxy-4-methyl-2-pentenyloxy)}-9,10-secopregna-5,7,10(19),16-tetraene ((*R*)-7g). Prepared according to the procedure for (*S*)-**7c**.[18] IR (neat): 3350, 2972, 2929, 2850, 1448, 1371, 1167, 1063 cm^{-1}; ^1H NMR (270 MHz, $CDCl_3$): δ 0.75 (s, 3H), 1.34 (s, 6H), 2.55–2.67 (m, 1H), 2.75–2.87 (m, 1H), 4.06 (q, J = 6.3 Hz, 1H), 4.11–4.30 (m, 3H), 4.38–4.50 (m, 1H), 5.01 (br s, 1H), 5.34 (br s, 1H), 5.45 (dt, J = 12.5, 5.3 Hz, 1H), 5.58 (m, 2H), 6.01 (d, J = 11.2 Hz, 1H), 6.37 (d, J = 11.2 Hz, 1H); MS (ESI): m/z 451 ($[M+Na]^+$); UV λ_{max}: 263 nm; HPLC t_R = 11.20 min (purity 98.5%, column A), HPLC t_R = 9.97 min (purity >99%, column B); HRMS Calcd for $C_{27}H_{40}O_4Na$: 451.2824. Found: 451.2809.

4.1.12. 1α,3β-Dihydroxy-20(*R*)-{(*E*)-(4-hydroxy-4-methyl-2-pentenyloxy)}-9,10-secopregna-5,7,10(19),16-tetraene ((*R*)-7h). Prepared according to the procedure for (*S*)-**7c**.[18] IR (neat): 3390, 2972, 2931, 2850, 1448, 1371, 1217, 1153, 1095, 1057 cm^{-1}; ^1H NMR (270 MHz, $CDCl_3$): δ 0.75 (s, 3H), 1.33 (s, 6H), 2.56–2.68 (m, 1H), 2.78–2.88 (m, 1H), 3.85–4.08 (m, 3H), 4.18–4.30 (m, 1H), 4.39–5.00 (m, 1H), 5.01 (br s, 1H), 5.34 (br s, 1H), 5.62 (br s, 1H), 5.73 (dt, J = 15.8, 5.3 Hz, 1H), 5.85 (d, J = 15.8 Hz, 1H), 6.11 (d, J = 11.2 Hz, 1H), 6.38 (d, J = 11.2 Hz, 1H); MS (ESI): m/z 451 ($[M+Na]^+$); UV λ_{max}: 263 nm; HPLC t_R = 11.45 min (purity 97.5%, column A), HPLC t_R = 9.84 min (purity >99%, column B); HRMS Calcd for $C_{27}H_{40}O_4Na$: 451.2824. Found: 451.2838.

4.1.13. 1α,3β-Dihydroxy-20((*S*)-hydroxy-9,10-secopregna-5,7,10(19),16-tetraene ((*S*)-7a). Prepared according to the procedure for (*S*)-**7c**.[18] IR (neat): 3350, 2929, 1369, 1053, 733 cm^{-1}; ^1H NMR (270 MHz, $CDCl_3$): δ 0.80 (s, 3H), 1.35 (d, J = 6.9 Hz, 3H), 2.78–2.88 (m, 1H), 4.18–4.48 (m, 3H), 5.01 (br s, 1H), 5.34 (s, 1H), 5.64 (br s, 1H), 6.10 (d, J = 11.2 Hz, 1H), 6.37 (d, J = 11.2 Hz, 1H); MS (ESI): m/z 353 ($[M+Na]^+$); UV λ_{max}: 264 nm; HPLC t_R = 12.02 min (purity 98.7%, column A), HPLC t_R = 8.99 min (purity >99%, column B); HRMS Calcd for $C_{21}H_{30}O_3Na$: 353.2093. Found: 353.2094.

4.1.14. 1α,3β-Bis(*tert*-Butyldimethylsilyloxy-20((*S*)-[2,3(*R*)–epoxypropoxy]-9,10-pregna-5,7,16-triene ((*S*)-15). To 1α,3β-Bis(*tert*-butyldimethylsilyloxy-20(*S*)-hydroxypregna-5,7,16-triene (*S*)-**13** (1 g, 1.79 mmol) in THF (10 mL) were added NaH (95%, 225 mg, 8.91 mmol) and 15-crown-5 (200 mg, 0.908 mmol) portionwise with stirring at room temperature. To the resulting suspension was added (*R*)-(−)-glycidyl tosylate (1.02 g, 4.47 mmol) dropwise at the same temperature with stirring and the mixture was refluxed for 8.5 h. After cooling to room temperature, to this mixture was added NaH (95%, 100 mg, 3.96 mmol) and the mixture was refluxed for 3 h. After cooling to room temperature, this reaction mixture was partitioned between ethyl acetate and H_2O. The organic layer washed with brine, dried ($MgSO_4$), and evaporated in vacuo, and the residue was purified by column chromatography (SiO_2, eluting with 10% ethyl acetate–hexane) to yield (*S*)-**15** (743 mg, 68%) as a colorless oil: IR (neat): 2952, 2928, 2896, 1252, 834 cm^{-1}; ^1H NMR (270 MHz, $CDCl_3$): δ 0.05 (s, 3H), 0.06 (s, 6H), 0.11 (s, 3H), 0.88 (s, 21H), 0.94 (s, 3H), 1.32 (d, J = 6.4 Hz, 3H), 2.63 (dd, J = 2.6, 5.0 Hz, 1H), 2.79 (dd, J = 4.3, 5.0 Hz, 1H), 2.74–2.91 (m, 1H), 3.09–3.16 (m, 1H), 3.45 (dd, J = 5.1, 11.2 Hz, 1H), 3.52 (dd, J = 3.6, 11.2 Hz, 1H), 3.70 (br s, 1H), 3.95–4.13 (m, 1H), 5.36–5.43 (m, 1H), 5.58–5.66 (m, 2H); MS (EI): m/z 615 (M^++1), 73 (100%); UV λ_{max}: 270, 281, 293 nm.

4.1.15. 1α,3β-Bis(*tert*-Butyldimethylsilyloxy-20(*R*)-[2,3(*R*)-epoxypropoxy]-9,10-pregna-5,7,16-triene ((*R*)-15). Prepared according to the procedure for (*S*)-**15** [using 1α,3β-bis(*tert*-butyldimethylsilyloxy)-20(*R*)-hydroxypregna-5,7,16-triene (*R*)-**13** (323 mg, 0.578 mmol); NaH (95%, 76 mg, 2.99 mmol); 15-crown-5 (71 mg, 0.325 mmol);

THF (3 mL); (*R*)-(−)-glycidyl tosylate (330 mg, 1.45 mmol)] to give (*R*)-**15** (240 mg, 68%) as a pale yellow oil: IR(neat): 2952, 2932, 2896, 2856, 1254, 836 cm^{-1}; ^1H NMR (270 MHz, $CDCl_3$): δ 0.05 (s, 3H), 0.07 (s, 6H), 0.11 (s, 3H), 0.84 (s, 3H), 0.88 (s, 18H), 0.94 (s, 3H), 1.35 (d, J = 6.6 Hz, 3H), 2.58 (dd, J = 2.6, 4.8 Hz, 1H), 2.79 (dd, J = 4.5, 4.8 Hz, 1H), 2.76–2.92 (m, 1H), 3.09–3.19 (m, 1H), 3.37 (dd, J = 5.9, 11.2 Hz, 1H), 3.65 (dd, J = 3.5, 11.2 Hz, 1H), 3.71 (br s, 1H), 3.97–4.13 (m, 1H), 5.35–5.44 (m, 1H), 5.61 (d, J = 5.4 Hz, 1H), 5.66 (s, 1H); MS (EI): *m*/*z* 614 (M^+), 425 (100%); UV λ_{max}: 269, 281, 293 nm.

4.1.16. 1α,3β-Bis(*tert*-butyldimethylsilyloxy-20(*S*)-(2(*S*)-hydroxy-propoxy)-pregna-5,7,16-triene ((*S*)-16). To a solution of (*S*)-**15** (181 mg, 0.294 mmol) in Et_2O (3 mL) was added $LiAlH_4$ (6 mg, 0.158 mmol) portionwise with stirring at 0 °C. After stirring the reaction mixture for 2 h at the same temperature, to this reaction mixture was added the solution of THF/H_2O (4:1, 5 ml). The organic layer was extracted with ethyl acetate, washed with brine, dried ($MgSO_4$), and evaporated in vacuo, and the residue was purified by column chromatography (SiO_2, eluting with 10% ethyl acetate–hexane) to yield (*S*)-**16** (166 mg, 92%) as a colorless oil: IR (neat): 3460, 2932, 2856, 1080 cm^{-1}; ^1H NMR (270 MHz, $CDCl_3$): δ 0.05 (s, 3H), 0.07 (s, 6H), 0.11 (s, 3H), 0.88 (s, 21H), 0.94 (s, 3H), 1.14 (d, J = 6.3 Hz, 3H), 1.32 (d, J = 6.3 Hz, 3H), 2.80–2.91 (m, 1H), 3.24 (dd, J = 7.9, 9.2 Hz, 1H), 3.32 (dd, J = 3.1, 9.2 Hz, 1H), 3.70 (br s, 1H), 3.87–.13 (m, 3H), 5.35-5.44 (m, 1H), 5.62 (s, 1H), 5.56–5.66 (m, 1H); MS (EI): *m*/*z* 616 (M^+), 427 (100%); UV λ_{max}: 269, 281, 293 nm.

4.1.17. 1α,3β-Bis(*tert*-butyldimethylsilyloxy-20(*R*)-(2(*R*)-hydroxy-propoxy)-pregna-5,7,16-tetraene ((*R*)-16). Prepared according to the procedure for (*S*)-**16** [using (*R*)-**15** (180 mg, 0.292 mmol); $LiAlH_4$ (11.3 mg, 0.298 mmol); Et_2O (3 mL)] to give (*R*)-**16** (175 mg, 97%) as a colorless oil: IR (neat): 3464, 2944, 2856, 1084 cm^{-1}; ^1H NMR (270 MHz, $CDCl_3$): δ 0.05 (s, 3H), 0.07 (s, 6H), 0.11 (s, 3H), 0.84 (s, 3H), 0.88 (s, 18H), 0.94 (s, 3H), 1.14 (d, J = 6.4 Hz, 3H), 1.33 (d, J = 6.6 Hz, 3H), 2.42 (d, J = 2.6 Hz, 1H), 2.80–2.93 (m, 1H), 3.18 (dd, J = 8.7, 9.0 Hz, 1H), 3.43 (dd, J = 3.1, 9.0 Hz, 1H), 3.70 (br s, 1H), 3.85–4.13 (m, 3H), 5.39 (dd, J = 2.6, 5.4 Hz, 1H), 5.61 (d, J = 5.6 Hz, 1H), 5.65 (s, 1H); MS (EI): *m*/*z* 616 (M^+), 73 (100%); UV λ_{max}: 271, 281, 294 nm.

4.1.18. 1α,3β-Bis(*tert*-butyldimethylsilyloxy-20(*S*)-(2-oxo-propoxy)-pregna-5,7,16-triene ((*S*)-17). To a solution of (*S*)-**16** (166 mg, 0.269 mmol) and 4-methylmorpholine 4-oxide (50 mg, 0.427 mmol) in CH_2Cl_2 (2 mL) were added molecular sieves 4 Å (50 mg). After stirring the reaction mixture for 20 min at room temperature, to this reaction mixture was added tetrapropylammonium perruthenate (5 mg, 0.0142 mmol). After stirring for 55 min at the same temperature and filtration through Celite, the filtrate was extracted with hexane, washed with H_2O, brine, dried ($MgSO_4$), and evaporated in vacuo, and the residue was purified by column chromatography (SiO_2, eluting with 10% ethyl acetate–hexane) to yield (*S*)-**17** (145 mg, 87%) as a colorless oil: IR (neat): 2952, 2928, 2856, 1720, 1084 cm^{-1}; ^1H NMR (270 MHz, $CDCl_3$): δ 0.05 (s, 3H), 0.06 (s, 6H), 0.11 (s, 3H), 0.88 (s, 21H), 0.94 (s, 3H), 1.37 (d, J = 6.4 Hz, 3H), 2.17 (s, 3H), 2.79–2.93 (m, 1H), 3.70 (br s, 1H), 3.88 (d, J = 17.1 Hz, 1H), 4.02 (d, J = 17.1 Hz, 1H), 3.94–4.13 (m, 2H), 5.34–5.44 (m, 1H), 5.62 (s, 1H), 5.56–5.67 (m, 1H); MS (EI): *m*/*z* 614 (M^+), 73 (100%); UV λ_{max}: 270, 281, 293 nm.

4.1.19. 1α,3β-Bis(*tert*-butyldimethylsilyloxy-20(*R*)-(2-oxo-propoxy)-pregna-5,7,16-triene ((*R*)-17). Prepared according to the procedure for (*S*)-**17** [using (*R*)-**16** (175 mg, 0.283 mmol); 4-methylmorpholine 4-oxide (60 mg, 0.516 mmol); CH_2Cl_2 (2 mL); molecular sieves 4 Å (56 mg); tetrapropylammonium perruthenate (5.3 mg, 0.0151 mmol)] to give (*R*)-**17** (148 mg, 85%) as a colorless oil: IR (neat): 2952, 2932, 2856, 1720, 1100 cm^{-1}; ^1H NMR (270 MHz, $CDCl_3$): δ 0.05 (s, 3H), 0.06 (s, 6H), 0.11 (s, 3H), 0.85 (s, 3H), 0.88 (s, 18H), 0.94 (s, 3H), 1.37 (d, J = 6.6 Hz, 3H), 2.17 (s, 3H), 2.79–2.93 (m, 1H), 3.70 (br s, 1H), 3.93 (d, J = 17.0 Hz, 1H), 4.01 (d, J = 17.0 Hz, 1H), 3.97–4.14 (m, 3H), 5.39 (dd, J = 2.6, 5.4 Hz, 1H), 5.61 (d, J = 5.4 Hz, 1H), 5.67 (s, 1H); UV λ_{max}: 271, 282, 294 nm.

4.1.20. 1α,3β-Bis(*tert*-butyldimethylsilyloxy-20(*S*)-(2-hydroxy-2-methylpropoxy)-pregna-5,7,16-triene ((*S*)-14b). To a solution of (*S*)-**17** (144 mg, 0.234 mmol) in THF (3 mL) was added 0.93 M-MeMgBr in THF (0.75 mL, 0.698 mmol) at 0 °C. After stirring the reaction mixture for 15 min at the same temperature, to this reaction mixture was added aqueous NH_4Cl, and extracted AcOEt, washed with H_2O, aqueous $NaHCO_3$, brine, dried ($MgSO_4$) , and evaporated in vacuo, and the residue was purified by column chromatography in silica (eluting with 10% ethyl acetate–hexane) to yield (*S*)-**14b** (113 mg, 76%) as a colorless oil. IR (neat): 3450, 2952, 2928, 2856, 1096, 836 cm^{-1}; ^1H NMR (270 MHz, $CDCl_3$): δ 0.05 (s, 3H), 0.06 (s, 6H), 0.11 (s, 3H), 0.88 (s, 21H), 0.94 (s, 3H), 1.19 (s, 3H), 1.20 (s, 3H), 1.32 (d, J = 6.4 Hz, 3H), 2.80–2.91 (m, 1H), 3.09 (d, J = 8.7 Hz, 1H), 3.27 (d, J = 8.7 Hz, 1H), 3.67–3,74 (m, 1H), 3.95 (q, J = 6.4 Hz, 1H), 3.80–4.12 (m, 1H), 5.39 (dd, J = 2.4, 5.4 Hz, 1H), 5.60 (s, 1H), 5.56–5.63 (m, 1H); MS (EI): *m*/*z* 630 (M^+), 73 (100%); UV λ_{max}: 271, 282, 294 nm.

4.1.21. 1α,3β-Bis(*tert*-butyldimethylsilyloxy-20(*R*)-(2-hydroxy-2-methylpropoxy)-pregna-5,7,16-triene ((*R*)-14b). Prepared according to the procedure for (*S*)-**14b** [using (*R*)-**17** (147 mg, 0.239 mmol); 0.93 M-MeMgBr in THF (0.80 mL, 0.744 mmol); THF (3 mL)] to give (*S*)-**14b** (134 mg, 89%) as a colorless oil: IR (neat): 3440, 2952, 2932, 2856, 1096, 836 cm^{-1}; ^1H NMR (270 MHz, $CDCl_3$): δ 0.05 (s, 3H), 0.06 (s, 6H), 0.10 (s, 3H), 0.84 (s, 3H), 0.88 (s, 18H), 0.93 (s, 3H), 1.20 (s, 6H), 1.32 (d, J = 6.6 Hz, 3H), 2.79–2.93 (m, 1H), 3.21 (d, J = 8.7 Hz, 1H), 3.26 (d, J = 8.7 Hz, 1H), 3.70 (br s, 1H), 3.94–4.14 (m, 2H), 5.39 (dd, J = 2.6, 5.4 Hz, 1H), 5.63 (s, 1H), 5.57–5.67 (m, 1H); MS (EI): *m*/*z* 498

(M^+-*t*-Bu, *t*-Bu, H_2O), 73 (100%); UV λ_{max}: 271, 282, 294 nm.

4.1.22. 1α,3β-Dihydroxy-20(*S*)-(2-hydroxy-2-methylpropoxy)-pregna-5,7,16-triene ((*S*)-18). To a solution of (*S*)-**14b** (82.1 mg, 0.130 mmol) in THF (3 mL) was added 1.0 M-TBAF in THF (0.8 mL, 0.8 mmol) at room temperature. After refluxing for 16 h, the reaction mixture was cooled to room temperature and extracted with AcOEt. The extract was washed with aqueous 5% HCl, aqueous $NaHCO_3$, brine, dried ($MgSO_4$), and evaporated in vacuo to leave a residue, which was purified by preparative TLC (developed with 10% EtOH in CH_2Cl_2) to yield (*S*)-**18** (47 mg, 90%) as a colorless oil: IR (neat): 3400, 2968, 2932, 1084, 1052 cm^{-1}; ^1H NMR (270 MHz, $CDCl_3$): δ 0.88 (s, 3H), 0.96 (s, 3H), 1.19 (s, 6H), 1.31 (d, J = 6.5 Hz, 3H), 2.73–2.85 (m, 1H), 3.08 (d, J = 8.7 Hz, 1H), 3.27 (d, J = 8.7 Hz, 1H), 3.75 (br s, 1H), 3.95 (q, J = 6.5 Hz, 1H), 5.44 (dd, J = 2.6, 5.4 Hz, 1H), 5.59 (s, 1H), 5.72 (d, J = 5.4 Hz, 1H); MS (EI): *m*/*z* 402 (M^+), 59 (100%); UV λ_{max}: 271, 282, 294 nm.

4.1.23. 1α,3β-Dihydroxy-20(*R*)-(2-hydroxy-2-methylpropoxy)-pregna-5,7,16-triene ((*R*)-18). Prepared according to the procedure for (*S*)-**18** [using (*R*)-**14b** (109 mg, 0.172 mmol); 1.0 M-TBAF in THF (1 mL, 1 mmol); THF (3 mL)] to give (*R*)-**18** (44 mg, 63%) as a pale yellow oil: IR (neat): 3392, 2968, 2932, 1098, 1060 cm^{-1}; ^1H NMR (270 MHz, $CDCl_3$): δ 0.83 (s, 3H), 0.95 (s, 3H), 1.19 (s, 6H), 1.32 (d, J = 6.4 Hz, 3H), 2.73–2.86 (m, 1H), 3.20 (d, J = 8.7 Hz, 1H), 3.24 (d, J = 8.7 Hz, 1H), 3.74 (br s, 1H), 3.95–4.10 (m, 1H), 5.44 (dd, J = 2.6, 5.4 Hz, 1H), 5.63 (s, 1H), 5.67–5.76 (m, 1H); MS (EI): *m*/*z* 312 ($M^+-HOCH_2C(CH_3)_2OH$), 59 (100%); UV λ_{max}: 271, 282, 293 nm.

4.1.24. 1α,3β-Dihydroxy-20(*S*)-(2-hydroxy-2-methylpropoxy)-9,10-secopregna-5,7,10(19),16-tetraene ((*S*)-7b). A solution of (*S*)-**18** (46 mg, 0.114 mmol) in EtOH (200 mL) was irradiated using a 400 W high-pressure mercury lamp through a Vycor filter at 0 °C for 4 min. The solution was then refluxed gently for 2 h and concentrated in vacuo to leave an oil. The crude product was submitted to three-stage preparative TLC purification: (1) 0.5 mm × 2 plates, developed twice with CH_2Cl_2/EtOH = 10:1, (2) 0.25 mm × 1 plate, developed four times with hexane/AcOEt/EtOH = 10:5:1, 3) 0.25 mm × 3 plates, developed five times with hexane/AcOEt/EtOH = 10:5:1 to give (*S*)-**7b** (3.6 mg, 8%) as a colorless foam: IR (neat): 3368, 2928, 1444, 1368, 1180, 1166, 1056 cm^{-1}; ^1H NMR (270 MHz, $CDCl_3$): δ 0.78 (s, 3H), 1.20 (s, 9 H), 1.31 (d, J = 6.5 Hz, 3 H), 2.55–2.66 (m, 1H), 2.75–2.87 (m, 1H), 3.07 (d, J = 8.7 Hz, 1H), 3.27 (d, J = 8.7 Hz, 1H), 3.93 (q, J = 6.5 Hz, 1H), 4.18–4.30 (m, 1H), 4.40–4.50 (m, 1H), 5.01 (s, 1H), 5.34 (s, 1H), 5.56 (s, 1H), 6.11 (d, J = 11.5 Hz, 1H), 6.37 (d, J = 11.5 Hz, 1H); MS (ESI): *m*/*z* 425 ($[M+Na]^+$); UV λ_{max}: 263 nm; HPLC t_R = 11.12 min (purity 97.0%, column A), HPLC t_R = 10.07 min (purity >99%, column B); HRMS Calcd for $C_{25}H_{38}O_4Na$: 425.2668. Found: 425.2666.

4.1.25. 1α,3β-Dihydroxy-20(*R*)-(2-hydroxy-2-methylpropoxy)-9,10-secopregna-5,7,10(19),16-tetraene ((*R*)-7b). A solution of (*R*)-**18** (40 mg, 0.0994 mmol) in EtOH (200 mL) was irradiated for 3.75 min. The mixture was treated according to the procedure for (*S*)-**7b**. The crude product was submitted to two-stage preparative TLC purification: 1) 0.5 mm × 2 plates, developed three times with CH_2Cl_2/EtOH = 15:1, (2) 0.25 mm × 2 plates, developed four times with hexane/AcOEt/EtOH = 10:5:1 to give (*R*)-**7b** (3.7 mg, 9%) as a colorless oil: IR (neat): 3376, 2928, 1442, 1370, 1180, 1166, 1056 cm^{-1}; ^1H NMR (270 MHz, $CDCl_3$): δ 0.75 (s, 3H), 1.20 (s, 9H), 1.32 (d, J = 6.4 Hz, 3H), 2.52–2.66 (m, 1H), 2.74–2.89 (m, 1H), 3.20 (d, J = 8.6 Hz, 1H), 3.26 (d, J = 8.6 Hz, 1H), 4.00 (q, J = 6.4 Hz, 1H), 4.19–4.31 (m, 1H), 4.39–4.52 (m, 1H), 5.01 (s, 1H), 5.34 (s, 1H), 5.61 (s, 1H), 6.10 (d, J = 11.3 Hz, 1H), 6.37 (d, J = 11.3 Hz, 1H); MS (ESI): *m*/*z* 425 ($[M+Na]^+$); UV λ_{max}: 263 nm; HPLC t_R = 11.16 min (purity 99.0%, column A), HPLC t_R = 9.82 min (purity >99%, column B); HRMS Calcd for $C_{25}H_{38}O_4Na$: 425.2668, Found: 425.2666.

4.1.26. 1α,3β-Dihydroxy-20(*S*)-[2(*R*)-hydroxy-3-methylbutyloxy]-pregna-5,7,16-triene ((*Sr*)-20). To 1α,3β-Bis-(*tert*-butyldimethylsilyloxy-20(*S*)-hydroxypregna-5,7,16-triene (*S*)-**13** (71.5 mg, 0.128 mmol) in toluene (4.5 mL) were added *tert*-BuOK (170 mg, 1.52 mmol) and dibenzo-18-crown-6 (32 mg, 0.0888 mmol) with stirring at room temperature. To the resulting suspension was added (*R*)-(−)-1,2-epoxy-3-methylbutane (0.13 mL, 1.24 mmol) dropwise at the same temperature with stirring and the mixture was refluxed for 1 h. After cooling to room temperature, the reaction mixture was extracted with Et_2O, washed with brine, dried ($MgSO_4$), and evaporated in vacuo to leave a residue, which was purified by preparative TLC (developed three times with hexane/CH_2Cl_2/AcOEt = 45:5:2) to yield the mixture including (*Sr*)-**19i** (26.8 mg). To the mixture in THF (1 mL) was added 1 M-TBAF in THF (0.4 mL, 0.4 mmol) at room temperature. After being heated to reflux for 12 h, this reaction mixture was extracted with AcOEt, washed with aqueous 1 M-HCl, aqueous $NaHCO_3$ and brine, dried ($MgSO_4$), and evaporated in vacuo, and the residue was purified by preparative TLC (developed twice with CH_2Cl_2/EtOH = 15:1) to yield (*Sr*)-**20** (12.0 mg, 23%) as a colorless oil. IR (neat): 3420, 2924, 1460, 1368, 1056 cm^{-1}; ^1H NMR (270 MHz, $CDCl_3$): δ 0.89 (s, 3H), 0.89 (d, J = 6.6 Hz, 6H), 0.98 (s, 3H), 1.32 (d, J = 6.6 Hz, 3H), 2.49–2.62 (m, 1H), 2.72–2.87 (m, 1H), 3.26–3.54 (m, 3H), 3.77 (br s, 1H), 3.93–4.18 (m, 2H), 5.41–5.50 (m, 1H), 5.63 (br s, 1H), 5.70–5.80 (m, 1H); MS (EI): *m*/*z* 312, 55 (100%); UV λ_{max}: 269, 280, 292 nm.

4.1.27. 1α,3β-Dihydroxy-20(*S*)-[2(*R*)-hydroxy-3-methylbutyloxy]-9,10-secopregna-5,7,10(19),16-tetraene ((*Sr*)-7i). A solution of (*Sr*)-**20** (12.0 mg, 0.0288 mmol) in EtOH (200 mL) was irradiated for 1.67 min. The mixture was treated according to the procedure for **7c** (*S*). The crude product was submitted to 2-stage preparative TLC purification: (1) 0.25 mm × 1 plate, developed once with hexane/AcOEt/EtOH=10:5:1, *2*) 0.25 mm × 0.5 plate, developed twice with CH_2Cl_2/EtOH=30:1 and then,

developed twice with CH_2Cl_2/EtOH=10:1 to give (*Sr*)-**7i** (1.45 mg, 12%) as a colorless oil. IR (neat): 3400, 2924, 1446, 1370, 1056 cm^{-1}; ^1H NMR (270 MHz, $CDCl_3$): δ 0.78 (s, 3H), 0.89 (d, J = 6.9 Hz, 3H), 0.97 (d, J = 6.9 Hz, 3H), 1.31 (d, J = 6.6 Hz, 3H), 2.54–2.67 (m, 1H), 2.74–2.90 (m, 1H), 3.25–3.53 (m, 4H), 3.95 (q, J = 6.6 Hz, 1H), 4.19–4.32 (m, 1H), 4.38–4.51 (m, 1H), 5.01 (s, 1H), 5.34 (s, 1H), 5.58 (s, 1H), 6.11 (d, J = 11.4 Hz, 1H), 6.37 (d, J = 11.4 Hz, 1H); MS (ESI): m/z 439 ($[M+Na]^+$); UV λ_{max}: 264 nm; HPLC t_R = 10.93 min (purity 95.4%, column A), HPLC t_R = 10.40 min (purity >99%, column B); HRMS Calcd for $C_{26}H_{40}O_4Na$: 439.2824. Found: 439.2838.

4.1.28. 1α,3β-Dihydroxy-20(*S*)-{2(*S*)-hydroxy-3-methylbutyloxy}-pregna-5,7,16-triene ((*Ss*)-20). Prepared according to the procedure for (*Sr*)-**20** [using(*S*)-**13** (97.9 mg, 0.175 mmol), toluene (6 mL), *tert*-BuOK (230 mg, 2.05 mmol), and dibenzo-18-crown-6 (45 mg, 0.125 mmol), and (*S*)-(+)-1,2-epoxy-3-methylbutane (0.18 mL, 1.72 mmol), 1 M-TBAF in THF (0.5 mL, 0.5 mmol), and THF (1.5 mL)] to give (*Ss*)-**20** (20.6 mg, 36%) as a colorless oil: IR (neat): 3416, 2924, 1462, 1370, 1196, 1056 cm^{-1}; ^1H NMR (270 MHz, $CDCl_3$): δ 0.88 (s, 3H), 0.90 (d, J = 6.9 Hz, 6H), 0.97 (s, 3H), 1.31 (d, J = 6.6 Hz, 3H), 2.72–2.86 (m, 1H), 3.10–3.24 (m, 1H), 3.39–3.53 (m, 2H), 3.77 (br s, 1H), 3.96 (q, J = 6.6 Hz, 1H), 4.00–4.16 (m, 1 H), 5.40–5.49 (m, 1H), 5.60 (br s, 1H), 5.68–5.80 (m, 1H); MS (EI): m/z 312, 55 (100%); UV λ_{max}: 269, 281, 292 nm.

4.1.29. 1α,3β-Dihydroxy-20(*S*)-[2(*S*)-hydroxy-3-methylbutyloxy]-9,10-secopregna-5,7,10(19),16-tetraene ((*Ss*)-7i). A solution of (*Ss*)-**20** (9.7 mg, 0.0233 mmol) in EtOH (200 mL) was irradiated for 1.67 min. The mixture was treated according to the procedure for (*Sr*)-**7i**. The crude product was submitted to two-stage preparative TLC purification: (1) 0.25 mm × 1 plate, developed twice with CH_2Cl_2/EtOH=20:1; (2) 0.25 mm × 0.5 plate, developed twice with hexane/AcOEt/EtOH = 10:5:1 to give (*Ss*)-**7i** (1.06 mg, 11%) as a colorless oil: IR (neat) 3400, 2928, 1444, 1368, 1056 cm^{-1}; ^1H NMR (270 MHz, $CDCl_3$): δ 0.78 (s, 3H), 0.90 (d, J = 6.9 Hz, 3H), 0.96 (d, J = 6.9 Hz, 3H), 1.31 (d, J = 6.6 Hz, 3H), 2.53–2.68 (m, 1H), 2.76–2.90 (m, 1H), 3.09–3.24 (m, 1H), 3.40–3.55 (m, 2H), 3.88–4.01 (m, 1H), 4.18–4.30 (m, 1H), 4.40–4.50 (m, 1H), 5.01 (s, 1H), 5.34 (s, 1H), 5.57 (s, 1H), 6.10 (d, J = 11.4 Hz, 1H), 6.37 (d, J = 11.4 Hz, 1H); MS (ESI): m/z 439 ($[M+Na]^+$); UV λ_{max}: 262 nm; HPLC t_R = 10.95 min (purity 96.3%, column A), HPLC t_R = 10.30 min (purity >99%, column B); HRMS Calcd for $C_{26}H_{40}O_4Na$: 439.2824. Found: 439.2831.

4.1.30. 1α,3β-Dihydroxy-20(*R*)-[2(*R*)-hydroxy-3-methylbutyloxy]-pregna-5,7,16-triene ((*Rr*)-20). Prepared according to the procedure for (*Sr*)-**20** [using (*R*)-**13** (69.7 mg, 0.125 mmol), toluene (4 mL), *tert*-BuOK (170 mg, 1.52 mmol), and dibenzo-18-crown-6 (22 mg, 0.0610 mmol), and (*R*)-(−)-1,2-epoxy-3-methylbutane (0.13 mL, 1.24 mmol), 1 M-TBAF in THF (0.2 mL, 0.2 mmol), and THF (1 mL)] to give (*Rr*)-**20** (9.4 mg, 20%) as a colorless oil: IR (neat): 3404, 2960, 2928, 1462, 1370, 1272, 1196, 1056 cm^{-1}; ^1H NMR (270 MHz, $CDCl_3$): δ 0.85 (s, 3H), 0.90 (d, J = 6.9 Hz, 3H), 0.97 (d, J = 6.9 Hz, 3H), 0.98 (s, 3H), 1.33 (d, J = 6.3 Hz, 3H), 2.49–2.61 (m, 1H), 2.74–2.87 (m, 1H), 3.21–3.35 (m, 1H), 3.39–3.56 (m, 2H), 3.78 (br s, 1H), 3.93–4.15 (m, 2H), 5.40–5.50 (m, 1H), 5.65 (br s, 1H), 5.70–5.81 (m, 1H); MS (EI): m/z 414 (M^+-H_2O), 312, 55 (100%); UV λ_{max}: 269, 281, 293 nm.

4.1.31. 1α,3β-Dihydroxy-20(*R*)-[2(*R*)-hydroxy-3-methylbutyloxy]-9,10-secopregna-5,7,10(19),16-tetraene ((*Rr*)-7i). A solution of (*Rr*)-**20** (8.5 mg, 0.0204 mmol) in EtOH (200 mL) was irradiated for 1.67 min. The mixture was treated according to the procedure for (*Sr*)-**7i**. The crude product was submitted to 2-stage preparative TLC purification: (1) 0.25 mm × 1 plate, developed twice with CH_2Cl_2/EtOH = 15:1, (2) 0.25 mm × 0.5 plate, developed twice with hexane/AcOEt/EtOH = 10:5:1 to give (*Rr*)-**7i** (0.4 mg, 5%) as a colorless oil: IR (neat): 3416, 2924, 1452, 1370, 1262, 1066 cm^{-1}; ^1H NMR (270 MHz, $CDCl_3$): δ 0.75 (s, 3H), 0.91 (d, J = 6.6 Hz, 3H), 0.97 (d, J = 6.6 Hz, 3H), 1.32 (d, J = 6.3 Hz, 3H), 2.55–2.67 (m, 1H), 2.77–2.88 (m, 1H), 3.21–3.33 (m, 1H), 3.36–3.57 (m, 2H), 3.92–4.06 (m, 1H), 4.19–4.30 (m, 1H), 4.40–4.50 (m, 1H), 5.01 (s, 1H), 5.34 (s, 1H), 5.60 (s, 1H), 6.10 (d, J = 11.4 Hz, 1H), 6.37 (d, J = 11.4 Hz, 1H); MS (ESI): m/z 439 ($[M+Na]^+$); UV λ_{max}: 263 nm; HPLC t_R = 10.93 min (purity 91.4%, column A), HPLC t_R = 10.18 min (purity >99%, column B); HRMS Calcd for $C_{26}H_{40}O_4Na$: 439.2824. Found: 439.2829.

4.1.32. 1α,3β-Dihydroxy-20(*R*)-[2(*S*)-hydroxy-3-methylbutyloxy]-pregna-5,7,16-triene ((*Rs*)-20). Prepared according to the procedure for (*Sr*)-**20** [using (*R*)-**13** (79.0 mg, 0.141 mmol), toluene (4.5 mL), *tert*-BuOK (190 mg, 1.69 mmol), and dibenzo-18-crown-6 (25 mg, 0.0694 mmol), and (*S*)-(+)-1,2-epoxy-3-methylbutane (0.15 mL, 1.43 mmol), 1 M-TBAF in THF (0.25 mL, 0.25 mmol), and THF (1 mL)] to give (*Rs*)-**20** (11.0 mg, 21%) as a colorless oil: IR (neat): 3416, 3036, 2928, 1462, 1370, 1270, 1196, 1056 cm^{-1}: ^1H NMR (270 MHz, $CDCl_3$): δ 0.84 (s, 3H), 0.90 (d, J = 6.9 Hz, 3H), 0.97 (d, J = 6.9 Hz, 3H), 0.97 (s, 3H), 1.34 (d, J = 6.6 Hz, 3H), 2.72–2.88 (m, 1H), 3.19–3.34 (m, 1H), 3.40–3.60 (m, 2H), 3.77 (br s, 1H), 3.93–4.16 (m, 2H), 5.40–5.50 (m, 1H), 5.67 (s, 1H), 5.71–5.80 (m, 1H); MS (EI): m/z 312, 55 (100%); UV λ_{max}: 270, 281, 293 nm.

4.1.33. 1α,3β-Dihydroxy-20(*R*)-[2(*S*)-hydroxy-3-methylbutyloxy]-9,10-secopregna-5,7,10(19),16-tetraene ((*Rs*)-7i). A solution of (*Rs*)-**20** (9.9 mg, 0.0238 mmol) in EtOH (200 mL) was irradiated for 1.67 min. The mixture was treated according to the procedure for (*Sr*)-**7i**. The crude product was submitted to 2-stage preparative TLC purification, (1) 0.25 mm × 1 plate, developed twice with hexane/AcOEt/EtOH = 10:5:1, (2) 0.25 mm × 0.5 plate, developed twice with CH_2Cl_2/EtOH=15:1 to give (*Rs*)-**7i** (0.786 mg, 8%) as a colorless oil: IR (neat): 3392, 2928, 1452, 1370, 1264, 1056 cm^{-1}; ^1H NMR (270 MHz, $CDCl_3$): δ 0.74 (s, 3H), 0.90 (d, J = 6.6 Hz, 3H), 0.97 (d, J = 6.6 Hz, 3H), 1.33 (d, J = 6.3 Hz, 3H), 2.55–2.68 (m,

1H), 2.77–2.90 (m, 1H), 3.21–3.34 (m, 1H), 3.41–3.56 (m, 2H), 3.98 (q, $J = 6.3$ Hz, 1H), 4.18–4.31 (m, 1H), 4.38–4.51 (m, 1H), 5.01 (s, 1H), 5.34 (s, 1H), 5.63 (s, 1H), 6.10 (d, $J = 11.4$ Hz, 1H), 6.37 (d, $J = 11.4$ Hz, 1H); MS (ESI): m/z 439 ($[M+Na]^+$); UV λ_{max}: 262 nm; HPLC $t_R = 10.91$ min (purity 98.7%, column A), HPLC $t_R = 10.30$ min (purity >99%, column B); HRMS: Calcd for $C_{26}H_{40}O_4Na$: 439.2824. Found: 439.2827.

4.2. In vitro human keratinocyte growth inhibition assay

Normal human epidermal keratinocytes (adult skin, passage 4, Cat# CC-2501, Clonetics) were plated in 96-well tissue culture plates (flat-bottom, Costar) at 1×10^3 cells/well in KGM-2 (Clonetics). After 4–6 h, the test compounds were added and the cells were cultured in KGM-2 (200 μL/well) for 3 days at 37 °C, 5% CO_2. 10 μL of [^{3}H]thymidine (7.4 kBq/well) was added and the cells were cultured at 37 °C, 5% CO_2 overnight. The cells were trypsinized and transferred to a glass filter. The [^{3}H]thymidine incorporation was measured by a liquid scintillation counter.

4.3. In vivo Ca effect (determination of blood ionized calcium levels)

Male BALB/c AnN Crj mice were housed individually in aluminum cages and received food and water ad libitum. After 1 week acclimation, back skin (about 2 cm × 1.5 cm) was shaved with a hair clipper and received 1000 μg/kg (2 mL/kg) of test compound. Blood was collected from the eyepit 2 days after the administration. Blood ionized calcium level was measured by pH/Ca^{2+} analyzer 634 (Bayer Corporation).

4.4. In vitro metabolic stability evaluation

Rat liver microsomes were prepared from untreated Sprague–Dawley rat liver according to the conventional method[25] in Chugai Pharmaceutical Co., Ltd. For some stability experiments, commercially available rat microsomes from XenoTech, LLC (KS, USA) were purchased and prepared using essentially the same method as discribed above. Incubation was carried out at 37 °C using an incubation mixture of 100 μg of rat liver microsomes, 0.1 μmol NADPH, and 100 μL of a 0.1 M phosphate buffer (pH 7.4) containing the test compounds in ethanol solution (final concn; 1 μM). Reactions were stopped after 15 and 30 min by addition of 100 μL methanol. After removal of protein precipitate by centrifugation, the supernatant (100 μL) was injected into the HPLC system. Microsomal elimination constants (k_e) of test compounds were calculated from concentrations of a residual compound at 0, 15, and 30 min.

4.5. In vivo pharmacokinetics study

Dosing solutions were prepared as a saline solution containing 2% Tween 80 and 1% ethanol at a concentration of 10 or 100 μg/mL. For OCT, [26-^{3}H]OCT was used as a saline solution containing 0.01% Tween 20 and 1% ethanol. Each solution was administered intravenously to SD rats (♂, 7–8wk) at a dose of 10 or 100 μg/kg. After an intravenous administration, blood samples were collected with time (0–24 hr) to prepare immediately plasma samples. Except for OCT, they were used as quantitation samples after liquid–liquid extraction. Plasma concentration of dosed compounds was quantified by HPLC (LC-10AD, Shimadzu, Japan) or LC–MS (Quattro II, Waters Ltd., UK) according to the method[26] of a vitamin D analog; OCT. For OCT, after methanol precipitation of plasma samples, radioactivities of OCT fractions were measured by liquid scintillation counter (LSC-900, Aloka, Japan). PK parameters were calculated by a non-compartment model using WinNonlin (Pharsight Corp., Mountain View, USA).

4.6. Molecular modeling

4.6.1. Preparation of molecules. Molecular modeling was performed with the SYBYL Molecular Modeling package version 6.9 running on a Linux workstation. Molecular docking experiments conducted on six of the vitamin D_3 analogs, **7g** and **7h**, with an unsaturated bond in the side-chain moiety, are listed in Table 2. Molecules were constructed in SYBYL6.9 (Tripos Inc., St. Louis, MO) based on several reported known vitamin D receptor (VDR) ligand complexes in the Protein Data Bank (PDB) and in-house complex coordinates (unpublished data). Gasteiger–Hückel charges were computed for ligand atoms. The docking study was carried out using the crystal structure of VDR with **1** resolved at 1.80 Å (PDB code: 1DB1). After removing all bound water molecules and **1** from the VDR complex, hydrogen atoms were added and Kollman charges were computed for VDR atoms. Three water molecules in the ligand-binding pocket were considered to be part of the protein. All hydrogen atoms were relaxed using 300 cycles of MMFF94s force field minimization implemented in SYBYL package.

4.6.2. DOCK 4.0.1 docking. Generation of docking poses of each ligand into the binding pocket was performed using DOCK version 4.0.1[27,28] in order to obtain an ensemble of initial geometries of the ligands. In order to collect diverse and stable docking poses, the option of flexible docking and torsion minimization was performed followed by relaxation of 250 simplex minimizations to a convergence of 0.1 kcal/mol.

4.6.3. MM-PBSA. Conformers generated from the docking experiments of the ligands were subjected to MM-PBSA calculation using AMBER version 7 software.[29] The initial complex within 20 Å from the ligand was soaked in a sphere of water .After AMBER minimization of 1000 cycles at 300 K, docking free-energy was evaluated using MM-PBSA calculations. The most stable docking poses of each ligand are shown in Figure 1.

Acknowledgments

We gratefully thank Dr. Kunio Ogasawara, Professor Emeritus, Tohoku University, for his helpful sugges-

tions. We also thank Dr. Bernd Kuhn, in F. Hoffmann-La Roche Ltd., for MM-PBSA calculation, Mr. Atsushi Matsuo for technical support of computational calculation, and Mr. Kenichiro Kotake, Ms. Ikumi Tanabe, and Ms. Miyuki Yagi for HRMS measurements of the compounds. We also wish to thank Mr. Toshiro Kozono, Mr.Tadakatsu Takahashi, Mr. Toru Esaki, Dr. Masayuki Ohmori, Mr. Takashi Emura, Mr. Kazutomo Kinoshita, Mr. Yoshiyuki Furuta, Mr. Nobuaki Kato, Mr. Tetsuya Mitsui, Mr. Tatsuhiko Tachibana, Mr. Yoshiaki Nabuchi, and Dr. Noboru Kubodera in Chugai Pharmaceutical Co., Ltd., for their advice and encouragement. We also acknowledge Ms. Frances Ford (Chugai) for her useful advice in the preparation and language editing of this paper.

References and notes

1. Tanaka, H.; Abe, E.; Miyaura, C.; Kuribayashi, T.; Konno, K.; Nishii, Y.; Suda, T. *Biochem. J.* **1982**, *204*, 713–719.
2. Bouillon, R.; Okamura, W. H.; Norman, A. W. *Endocr. Rev.* **1995**, *16*, 200–257.
3. Murayama, E.; Miyamoto, K.; Kubodera, N.; Mori, T.; Matsunaga, I. *Chem. Pharm. Bull.* **1986**, *34*, 4410–4413.
4. Morisaki, M.; Koizumi, N.; Ikekawa, N.; Takeshita, T.; Ishimoto, S. *J. Chem. Soc., Perkin Trans. 1* **1975**, 1421–1424.
5. Binderup, L.; Bramm, E. *Biochem. Pharmacol.* **1988**, *37*, 889–895.
6. Naveh-Many, T.; Silver, J. *Endocrinology* **1993**, *133*, 2724–2728.
7. Ishigai, M.; Arai, S.; Ishitani, Y.; Kumaki, K. *J. Steroid Biochem. Mol. Biol.* **1998**, *66*, 281–293.
8. Kobayashi, T.; Okano, T.; Tsugawa, N.; Masuda, S.; Takeuchi, A.; Nishii, Y. *Contrib. Nephrol.* **1991**, *91*, 129–133.
9. Masuda, S.; Byford, V.; Kremer, R.; Makin, H. L.; Kubodera, N.; Nishii, Y.; Okazaki, A.; Okano, T.; Kobayashi, T.; Jones, G. *J. Biol. Chem.* **1996**, *271*, 8700–8708.
10. Lee, H. J.; Soliman, M. R. *Science* **1982**, *215*, 989–991.
11. Bodor, N. *Med. Res. Rev.* **1984**, *4*, 449–469.
12. Werz, O.; Wiesinger, H.; Steinmeyer, A.; Steinhilber, D. *Biochem. Pharmacol.* **2000**, *59*, 1597–1601.
13. Ferrara, J.; McCuaig, K.; Hendy, G. N.; Uskokovic, M.; White, J. H. *J. Biol. Chem.* **1994**, *269*, 2971–2981.
14. Vyas, K. P.; Kari, P. H.; Wang, R. W.; Lu, A. Y. *Biochem. Pharmacol.* **1990**, *39*, 67–73.
15. Wang, R. W.; Kari, P. H.; Lu, A. Y.; Thomas, P. E.; Guengerich, F. P.; Vyas, K. P. *Arch. Biochem. Biophys.* **1991**, *290*, 355–361.
16. Greenspan, M. D.; Yudkovitz, J. B.; Alberts, A. W.; Argenbright, L. S.; Arison, B. H.; Smith, J. L. *Drug Metab. Dispos.* **1988**, *16*, 678–682.
17. Zhang, H.; Coville, P. F.; Walker, R. J.; Miners, J. O.; Birkett, D. J.; Wanwimolruk, S. *Br. J. Clin. Pharmacol.* **1997**, *43*, 245–252.
18. Kawase, A. JP Patent 10-231284, 1998.
19. Shimizu, H.; Shimizu, K.; Kubodera, N.; Yakushijin, K.; Horne, D. A. *Tetrahedron Lett.* **2004**, *45*, 1347–1350.
20. Shimizu, H.; Shimizu, K.; Kubodera, N.; Yakushijin, K.; Horne, D. A. *Heterocycles* **2004**, *63*, 1335–1343.
21. Shimizu, H.; Shimizu, K.; Kubodera, N.; Mikami, T.; Tsuzaki, K.; Suwa, H.; Harada, K.; Hiraide, A.; Shimizu, M.; Koyama, K.; Ichikawa, Y.; Hirasawa, D.; Kito, Y.; Kobayashi, M.; Kigawa, M.; Kato, M.; Kozono, T.; Tanaka, H.; Tanabe, M.; Iguchi, M.; Yoshida, M. *Org. Proc. Res. Devel.* **2005**, *9*, 278–287.
22. Nagpal, S.; Lu, J.; Boehm, M. F. *Curr. Med. Chem.* **2001**, *8*, 1661–1679.
23. Bishop, J. E.; Collins, E. D.; Okamura, W. H.; Norman, A. W. *J. Bone Miner. Res.* **1994**, *9*, 1277–1288.
24. Takeyama, K.; Masuhiro, Y.; Fuse, H.; Endoh, H.; Murayama, A.; Kitanaka, S.; Suzawa, M.; Yanagisawa, J.; Kato, S. *Mol. Cell Biol.* **1999**, *19*, 1049–1055.
25. Funae, Y.; Imaoka, S. *Biochim. Biophys. Acta* **1985**, *842*, 119–132.
26. Ishigai, M.; Asoh, Y.; Kumaki, K. *J. Chromatogr., B. Biomed. Sci. Appl.* **1998**, *706*, 261–267.
27. Case, D. A.; Pearlman, D. A.; Caldwell, J. W.; Cheatham III, T. E.; Wang, J.; Ross, W. S.; Simmerling, C. L.; Darden, T. A.; Merz, K. M.; Stanton, R. V.; Cheng, A. L.; Vincent, J. J.; Crowley, M.; Tsui, V.; Gohlke, H.; Radmer, R. J.; Duan, Y.; Pitera, J.; Massova, I.; Seibel, G. L.; Singh, U. C.; Weiner, P. K.; Kollman, P. A.; AMBER 7, 2002.
28. Kuntz, I. D.; Blaney, J. M.; Oatley, S. J.; Langridge, R.; Ferrin, T. E. *J. Mol. Biol.* **1982**, *161*, 269–288.
29. Kuhn, B.; Gerber, P.; Schulz-Gasch, T.; Stahl, M. *J. Med. Chem.* **2005**, *48*, 4040–4048.